Effects of Drilling Degrees of Freedom in the Finite Element Modeling of P- and SV-wave Scattering Problems

*Jae-Hwan Kim

* The present work was supported by Inha university research fund in 1997. The support is gratefully acknowledged.

Abstract

This paper deals with a hybrid finite element method for wave scattering problems in infinite domains. Scattering of waves involving complex geometries, in conjunction with infinite domains is modeled by introducing a mathematical boundary within which a finite element representation is employed. On the mathematical boundary, the finite element representation is matched with a known analytical solution in the infinite domain in terms of fields and their derivatives. The derivative continuity is implemented by using a slope constraint. Drilling degrees of freedom at each node of the finite element model are introduced to make the numerical model more sensitive to the transverse component of the elastodynamic field. To verify the effects of drilling degrees freedom and slope constraints individually, reflection of normally incident P and SV waves on a traction free half spaces is considered. For the P-wave incidence, the results indicate that the use of slope constraint is more effective because it suppresses artificial reflection at the mathematical boundary. For the SV-wave case, the use of drilling degrees freedom is more effective by reducing numerical error at irregular frequencies.

Ⅰ. Introduction

Numerical modeling of wave propagation and scattering in infinite domain has been of interest in many fields. There are several numerical approaches which have been used to treat wave problems in infinite domains involving complex geometries. The first one is the well-known boundary element method (BEM) [1,2]. This approach has been widely used in radiation and scattering of waves. However, a major drawback of BEM is that it does not have a unique solution at irregular frequencies. Attempts have been made to remove the irregular frequencies in many ways [3-5]. An alternative method is to use an infinite element [6]. Finite element can be used for the inner region and the infinite elements can account for effects of the outer region. Another method is the so-called matching technique [7] that uses finite element method in a finite region and analytical solutions to obtain the boundary conditions for this finite element model. T-matrix method [8] can also be used in conjunction with the finite element method. The notable feature of this approach is the absence of spurious peaks due to the implementation of the extinction or null field equation and the excellent agreement with experimental results.

The introduction of an absorbing boundary condition (ABC) minimizes non-physical reflection from the mathematical boundary (Figure 1) [9-10]. The basis idea of the ABC operator method is to map the Sommerfeld radiation condition from the farfield to the near-farfield with less truncation error and lower reflection. Recently, Givoli and Keller [12] and Harari and Hughes [13] derived

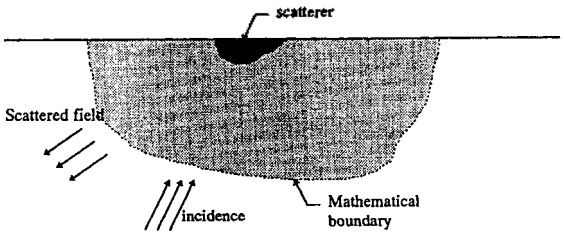

Figure 1. Semi-infinite domain problem.

* Department of Mechanical Engineering Inha Univerisity
Manuscript Received : March 2, 1999

exact non-local type non-reflecting boundary conditions, so called to Dirichlet-to-Neumann boundary condition, or DtN boundary condition. However, when the DtN operator is truncated for implementation, uniqueness is lost at characteristic frequencies.

The finite element method has been widely used in investigating wave propagation and scattering problems because it can be used for inhomogeneous and anisotropic materials and complex geometries. Since the finite element technique is an approximation technique, it has some limitations. Dispersion and spurious oscillation phenomena in finite element solutions have been investigated [14]. However, the effects of displacement-based conventional finite elements are rarely investigated. There are basically three kinds of fields; irrotational acoustic fields, solenoidal electromagnetic fields and elastodynamic fields which have both irrotational and solenoidal components. For acoustic fields, the use of conventional finite element representations for nodal displacements is sufficient. For solenoidal fields, it has been found that node-based classical finite elements have drawbacks [15]. Vector fields have tangential continuity across all surfaces whereas their normal components have a discontinuity across a material interface. Representations of solenoidal fields as piece-wise linear, continuous, functions of space are not adequate. Such representations are too rigid across interfaces and result in loss of accuracy in computations.

Recently, Kim et al. [16] proposed the use of drilling degrees of freedom (d.o.f.) in addition to nodal displacements in the finite element approximation to take into account the solenoidal component of the elastic field more precisely. For further transparency at the mathematical boundary, the continuity of all derivatives are introduced via a penalty method. It is found that by using slope constraint on the mathematical boundary and introducing drilling d.o.f. at the finite element nodes, the error due to artificial reflection can be reduced remarkably. It was also observed that this approach minimized the effect of resonance frequencies associated with the mathematical domain as the frequency of the exciting wave increased and wavelengths became much smaller than the size of the numerical domain. However, the individual roles of the drilling d.o.f. and the slope constraint could not be clearly inferred because oblique incidence of P-wave was considered in that work.

In this paper we study the individual effects of slope constraint and drilling d.o.f. in the finite element modeling of wave scattering problems associated with infinite domains. Instead of oblique incidence, normal incidence is considered because at normal incidence there is no mode conversion at the traction free boundary of the halfspace. Normal incidence of SV-waves is also considered and new insights are obtained as to the roles of drilling d.o.f. and slope constraints.

II. Finite element formulation

The finite element formulation in this paper is not much different from the conventional formulation for elastodynamic problems except for the use of drilling degrees of freedom and slope constraints. Details of the formulation may be found in [16] and a brief summary will be presented here.

2.1. Drilling degrees of freedom

Rotational degrees of freedom at corner nodes of finite elements are considered to alleviate the stiff behavior of linear finite element in bending motion. Figure 2 shows a linear element with drilling d.o.f. in the two-dimensional case.

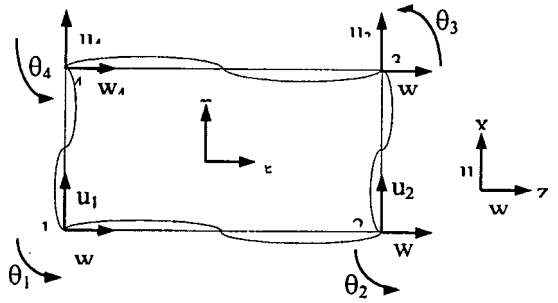

Figure 2. Linear element with drilling d.o.f.

From the nodal values, the displacement can be represented as follows by using proper interpolation functions:

$$\mathbf{u}=\begin{Bmatrix} w \\ u \end{Bmatrix}=\mathbf{N}_i\hat{\mathbf{u}}=\begin{bmatrix} N_1 & 0 & N_5 & N_2 & 0 & N_6 & N_3 & 0 & N_7 & N_4 & 0 & N_8 \\ 0 & N_1 & N_9 & 0 & N_2 & N_{10} & 0 & N_3 & N_{11} & 0 & N_4 & N_{12} \end{bmatrix}\begin{Bmatrix} w_1 \\ u_1 \\ \theta_1 \\ \vdots \end{Bmatrix} \tag{1}$$

where N_1-N_4 are conventional interpolation functions for linear elements and N_5-N_{12} are the functions that incorporate displacement and drilling d.o.f. A detailed procedure to derive these relationships is given in [16] and the derived shape functions are in Appendix A.

The drilling d.o.f. are simply rotations each axis. In the two-dimensional case, the axis of rotation is the y-axis.

The physical rotation in a continuum, Ω, is defined as

$$\Omega_y = \frac{1}{2}\left(-\frac{\partial v}{\partial x}+\frac{\partial u}{\partial z}\right) = \mathbf{B}_\omega \hat{\mathbf{u}} . \tag{2}$$

Since the rotation of drilling d.o.f. should be the physical rotation, a penalty factor γ is used to enforce the equality of θ and Ω,

$$J_\omega = \frac{1}{2}\gamma \int (\Omega-\theta)^2 dv \tag{3}$$

where θ is the rotation of drilling d.o.f.

$$\theta = \omega_y = N_\gamma \hat{u} \tag{4}$$

and

$$\mathbf{N}_\gamma = \begin{bmatrix} 0 & 0 & N_1 & 0 & 0 & N_2 & 0 & 0 & N_3 & 0 & 0 & N_4 \end{bmatrix} . \tag{5}$$

2.2. Continuity of derivatives of the fields at the mathematical boundary

To eliminate spurious resonance frequencies associated with the resonance frequencies associated with the mathematical boundary, one can impose continuity of displacement fields and their derivatives on the mathematical boundary. The purpose is to render the mathematical boundary to be transparent or non-reflecting. The slope constraints that has to be imposed on the mathematical boundary may be written as

$$\frac{\partial u}{\partial x} = \bar{u}_\Gamma \qquad on \Gamma \tag{6}$$

where Γ is the mathematical boundary, x=[x, z]. On the right side of above equation, $\mathbf{u}_\Gamma$ is a known solution for the field outside the mathematical domain. On the left side, $\mathbf{u}$, and its derivatives are obtained from the finite element model. This approach works in cases where the scatterer is very small compared to the size of the mathematical domain and/or the solution outside the domain is the equal to that in the absence of the scatterer or inhomogeneity.

In terms of interpolation functions, the nodal derivatives on the mathematical boundary may be written as:

$$\frac{\partial u}{\partial x} = \begin{Bmatrix} \partial w/\partial z \\ \partial w/\partial x \\ \partial u/\partial x \\ \partial u/\partial z \end{Bmatrix} = \begin{bmatrix} \partial/\partial z & 0 \\ \partial/\partial x & 0 \\ 0 & \partial/\partial z \\ 0 & \partial/\partial x \end{bmatrix} \begin{Bmatrix} w \\ u \end{Bmatrix} = B_n \hat{u} \tag{7}$$

By using the penalty factor α, we can express the integral relation for the slope constraints as

$$J_\alpha = \frac{\alpha}{2}\int_\Gamma \left\{\frac{\partial u}{\partial x}-\bar{u}_\Gamma\right\}^2 d\Gamma \tag{8}$$

For the finite element formulation of elastodynamic problems, Hamilton' s principle can be invoked.

$$J = \int_{t_1}^{t_2} \{T - V + B_E\} dt \tag{9}$$

For the finite element equations, eq. (9) most be modified by combining (3) and (8),

$$J^* = J + J_\omega + J_\alpha \tag{10}$$

If we assume that this is the steady state case and after performing a first variation, the final form of the finite element equations becomes

$$\left\{-\omega^2[\mathbf{M}]+[\mathbf{K}+\gamma \mathbf{K}_\omega+\alpha \mathbf{K}_\Gamma]\right\}\{\hat{\mathbf{U}}\} = \{\hat{\mathbf{F}}+\alpha \mathbf{F}_\Gamma\} \tag{11}$$

where **M**, **K** are mass and stiffness matrices of the elastic medium, and

$$\mathbf{K}_\Gamma = \int_\Gamma \mathbf{B}_n^T \mathbf{B}_n d\Gamma , \tag{12}$$

$$\mathbf{F}_\Gamma = \int_\Gamma \bar{\mathbf{u}}_\Gamma^T \mathbf{B}_n d\Gamma , \tag{13}$$

$$\mathbf{K}_\omega = \int \left[\mathbf{B}_\omega - \mathbf{N}_\gamma\right]^T \left[\mathbf{B}_\omega - \mathbf{N}_\gamma\right] dV \tag{14}$$

where ω is the excitation frequency. Boundary conditions for $\mathbf{u}$ and their derivatives $\mathbf{u}_\Gamma$ are calculated form the analytical solution of the plane-wave problem.

2.3. Analytical solution of plane-wave problem

To obtain an analytical representation for the fields in the infinite domain, the problem of plane-wave scattering in the half space in the absence of any structure is considered (Figure 3). The hypothesis is that even in the presence of the structure, if the mathematical domain is much larger than the structure, the plane-wave nature of

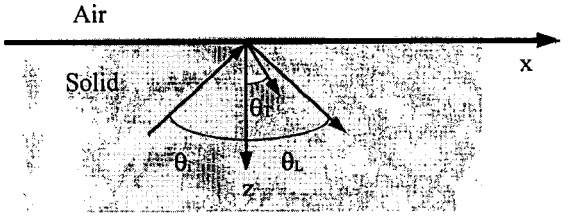

Figure 3. Semi-infinite elastic domain problem.

the solution will be maintained.

Accordingly, we consider a semi-infinite elastic domain with P- and SV-wave incidences, respectively. The incidence fields of P- or SV-wave can be represented as

$$\mathbf{u}_i=\mathbf{p}_i A_i \exp(j\mathbf{k}_i \cdot \mathbf{r}) \quad (15)$$

where $\mathbf{p}_i$ is the polarization vector of the incidence,

$$\mathbf{p}_i=-\cos\theta_i \mathbf{e}_z+\sin\theta_i \mathbf{e}_x, \quad \text{for P incidence} \quad (16)$$
$$\mathbf{p}_i=-\sin\theta_i \mathbf{e}_z-\cos\theta_i \mathbf{e}_x, \quad \text{for SV incidence} \quad (17)$$

$\mathbf{k}_i$ is the wave vector of the incidence,

$$\mathbf{k}_i=k_L(-\cos\theta_i \mathbf{e}_z+\sin\theta_i \mathbf{e}_x), \quad \text{for P incidence} \quad (18)$$
$$\mathbf{k}_i=k_T(-\cos\theta_i \mathbf{e}_z+\sin\theta_i \mathbf{e}_x), \quad \text{for SV incidence} \quad (19)$$

k_L and k_T are the wave numbers for P-wave and SV-wave respectively, and θ_i is incidence angle. The reflected waves at the top surface can be written as,

$$\mathbf{u}_r=\mathbf{p}_L A_L \exp(j\mathbf{k}_L \cdot \mathbf{r})+\mathbf{p}_T A_T \exp(j\mathbf{k}_T \cdot \mathbf{r}) \quad (20)$$

where $\mathbf{p}_L$ and $\mathbf{p}_T$ are the polarization vectors for P and SV waves respectively,

$$\mathbf{p}_L = \cos\theta_L \mathbf{e}_z+\sin\theta_L \mathbf{e}_x \quad (21)$$
$$\mathbf{p}_T = \cos\theta_T \mathbf{e}_z+\sin\theta_T \mathbf{e}_x . \quad (22)$$

$\mathbf{k}_L$ and $\mathbf{k}_T$ are the wave vectors for longitudinal and transverse waves respectively,

$$\mathbf{k}_L = k_L(\cos\theta_L \mathbf{e}_z+\sin\theta_L \mathbf{e}_x) \quad (23)$$
$$\mathbf{k}_T = k_T(\cos\theta_T \mathbf{e}_z+\sin\theta_T \mathbf{e}_x) \quad (24)$$

And, $\mathbf{r} = x\mathbf{e}_x + z\mathbf{e}_z$. By superimposing the incident and reflected waves, displacements in the solid region can be written as

$$\mathbf{u} = \mathbf{u}_i + \mathbf{u}_r = \mathbf{p}_i A_i \exp(j\,\mathbf{k}_i \cdot \mathbf{r}) + \mathbf{p}_L A_L \exp(j\,\mathbf{k}_L \cdot \mathbf{r}) + \mathbf{p}_T A_T \exp(j\,\mathbf{k}_T \cdot \mathbf{r}) \quad (25)$$

where A_i is the amplitude of incidence, θ_i is the angle of incidence, and the time factor, $\exp(j\omega t)$ is contained all fields, but omitted for convenience. A_L and A_T are amplitudes of longitudinal and transverse waves, respectively. $\mathbf{e}_x$, $\mathbf{e}_y$, $\mathbf{e}_z$ are the unit normal vectors in rectangular coordinates.

Snell's law gives the following relations that put the above equations in much simpler forms,

$$k_L \sin\theta_L = k_T \sin\theta_T = k_i \sin\theta_i \quad (26)$$

where k_i is incidence wave number, which is k_L for P-wave incidence and k_T for SV-wave incidence.

The boundary conditions at the top surface are

$$\text{at } z=0, \quad \tau_{zz}=0, \quad \tau_{xz}=0 \quad (27)$$

Thus, two unknown amplitudes, A_L, A_T can be found from the boundary conditions. Once the unknown amplitudes are found, after substituting these unknowns into Eq.(25), we can obtain the displacement at a desired location, say, at the mathematical boundary of the finite element model.

III. Numerical examples

An elastic half space problem is considered to prove the efficiency of enforcing slope constraints and endowing the finite elements with drilling d.o.f. to realize a transparent mathematical boundary (Figure 4). P and SV-wave incidences are considered and a finite element model is chosen such that the finite region will be solved with proper boundary conditions. In this problem, any specific scatterer is not considered in the model and the reflection at the top surface of the model, which is traction free boundary is taken into account.

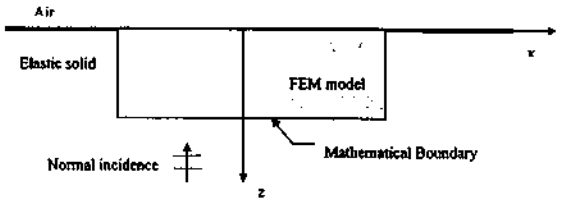

Figure 4. Elastic half space problem.

Parameters used in the analysis are as follows: elastic modulus of the medium E = 24×10^6 kPa, density of the medium $\rho = 2400\ kg/m^3$, Poisson ratio $\nu = 1/3$. Longitudinal wave speed in the medium $c_p = 3872\ m/s$ and the height and width of the finite element model is 200m and 600m, respectively. A four node linear element with drilling d.o.f. was used and 341 nodes are made. Constraint parameters for the slope constraint and drilling

d.o.f. are searched by an optimization technique at each frequency. To judge the finite element analysis results, the average error has been defined in the previous study as [16]

$$\text{Error} = \frac{1}{n}\sum_{i=1}^{n}\frac{|U_{FEM,i} - U_{Theory,i}|}{|U_{Theory,i}|} \tag{28}$$

This is for oblique incidence of P-wave. However, in normal incidence case, for example, P-wave normal incidence, the theoretical value of x displacement is zero. When SV-wave is normally impinging, in contrast, the theoretical y displacement is zero. These turns out the error defined in (28) to be infinite. Thus, the error criterion is slightly changed as follows,

$$\text{Error} = \frac{1}{n}\sum_{i=1}^{n}\frac{|W_{FEM,i} - W_{Theory,i}| + |u_{FEM,i}|}{A_i}$$

for P-normal incidence (29)

and

$$\text{Error} = \frac{1}{n}\sum_{i=1}^{n}\frac{|u_{FEM,i} - u_{Theory,i}| + |w_{FEM,i}|}{A_i}$$

for SV-normal incidence (30)

where $U_{FEM,i}=[w,\ u]_{FEM,i}$ is the displacement found from the finite element analysis and $U_{Theory,i}=[w,\ u]_{Theory,i}$ is the plane-wave solution at node I. Here, n is the number of nodes.

3.1. P-normal incidence

To distinguish the effects of drilling d.o.f. and slope constraints, P and SV-normal incidences are considered separately. P-waves generate particle movement in propagation direction. When P-waves are normally on a flat surface, P-waves are reflected normal to the surface . Thus, for normally incident P-waves, there is no mode conversion to SV-waves as in the case of oblique incidence. The same applies to normal incidence of SV-waves.

When the displacements are specified at the mathematical boundary and in the absence of slope constraints and the use of drilling d.o.f., spurious peaks are observed (original case in Figure 5). These peaks coincide with the natural frequencies of the rectangular slab associated with the mathematical domain.

When the slope constraints are enforced at the mathematical boundary, these irregular frequencies are suppressed completely (slope constraint case in Figure 5). This reduction is comparable with the oblique incidence case [16]. In the oblique incidence case, the peaks in the curves were shifted down considerably but the errors were still high and irregular frequencies are still present. This reduction shows that the use of slope constraints helps to reduce the artificial reflections at the irregular frequencies of the model. The penalty factor, α is searched optimally and its range is 10^{10}-10^{14}.

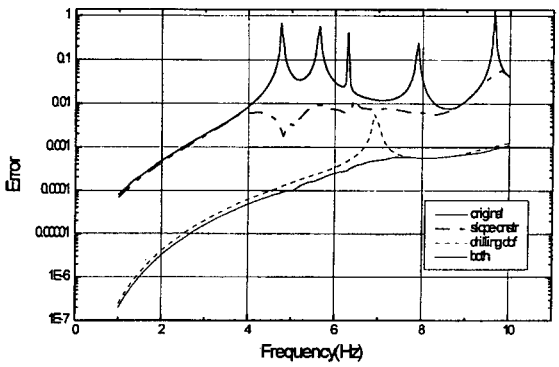

Figure 5. P-normal incidence case.

Next, the slope constraint and drilling d.o.f. are used simultaneously to eliminate artificial reflection. It is found that the error is reduced remarkably and at the same time, the peaks are completely eliminated (both case in Figure 5). This shows that slope constraint tends to eliminate irregular frequency while drilling d.o.f. reduce the error bound.

With the four-node linear finite element, drilling d.o.f. are used at each node without slope constraint. The rotational parameter, γ is in the range of 10^{15}-10^{18} . It is found that the error as well as the number of peaks are reduced (drilling d.o.f. case in Figure 5). The error reduction is due to the fact that the use of drilling d.o.f. avoids the stiff behavior of nodal-displacement-based finite elements. The decrease of the number of peaks in error curve might be caused from strong enforcement of the rotational constraint parameter. For comparison, the range of the rotational parameter, γ for oblique incidence of P-wave was 10^{4}-10^{6} , which is much less then that for normal P-wave incidence.

3.2. SV-normal incidence

For SV-wave, the particle motion is perpendicular to the direction of wave propagation. When SV-waves are incident normal to an elastic half space, only SV-waves are reflected. However, in contrast with normal incidence of P-wave, SV-waves travel similar to bending waves. In

other words, while normal P-wave produces compression or tension in the finite elements, SV-waves produce bending motion also. To take this into account, finite elements need to be more flexible, which implies that the role of drilling d.o.f. may be more important when shear waves are involved.

In Figure 6, original refer to the case when only displacement is specified at the mathematical boundary in the absence of slope constraint and drilling d.o.f. Several peaks are observed in the error curve. When slope constraints are imposed on the mathematical boundary, the first peak in the error curve is reduced, but other peaks still remained (slope constraint case in Figure 6). The range of the penalty factor, α is 10^7-10^9. However, by using drilling d.o.f. at each node without slope constraint, the peaks are nearly eliminated and the level of error is shifted down (drilling d.o.f. case in Figure 6). The range of rotational parameter, γ is 10^3-10^5. When the slope constraint and drilling d.o.f. are used at the same time, no further improvement is observed. Thus, from these results, we can conclude that the use of drilling d.o.f. in modeling shear wave propagation is more effective than for case of P-wave propagation. We may conclude that the use of drilling d.o.f. in conjunction with nodal displacements in finite element modeling of elastodynamic problems is an effective approach to take into account the solenoidal component of the elastic field more precisely.

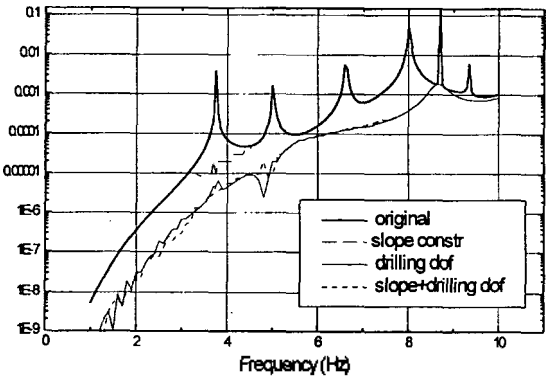

Figure 6. SV-normal incidence case.

Ⅳ. Conclusions

To model semi-infinite domain problems, the region is subdivided by introducing a mathematical boundary and the finite element method is used in the bounded region. When only displacement continuity is specified at the mathematical boundary, irregular frequencies lead to spurious peaks in the numerical solution. To suppress artificial reflections at the mathematical boundary, slope constraint are used on the mathematical boundary and drilling d.o.f are introduced at the finite element nodes. For normally incident P-waves, the use of slope constraints completely eliminates spurious peaks. For normally incident SV-waves, the introduction of drilling d.o.f. alone eliminates error peaks. This proves that the use of slope constraint is important in longitudinal wave propagation and the use of drilling d.o.f. takes into account transverse wave propagation more effectively. It also appears that for infinite domain problems, the use of an artificial boundary, exterior to which an analytical or series representation of the field is known, is an effective approach and complementary to the sue of absorbing condition, infinite elements or DtN boundary conditions.

APPENDIX A. shape functions associates with drilling d.o.f.

$$N_5=-\frac{L}{16}(1-\eta)(1+\eta)(1-\xi), \qquad N_9=\frac{L}{16}(1-\eta)(1+\xi)(1-\xi),$$

$$N_6=-\frac{L}{16}(1-\eta)(1+\eta)(1-\xi), \qquad N_{10}=-\frac{L}{16}(1-\eta)(1-\xi)(1+\xi)$$

$$N_7=-\frac{L}{16}(1-\eta)(1+\eta)(1+\xi), \qquad N_{11}=\frac{L}{16}(1+\eta)(1-\xi)(1+\xi)$$

$$N_8=-\frac{L}{16}(1-\eta)(1+\eta)(1-\xi), \qquad N_{12}=\frac{L}{16}(1+\eta)(1+\xi)(1-\xi)$$

References

1. C.A. Brebbia, The Boundary Element Method for Engineers, Wiley, New York ,1980
2. D.T.Wilton, Acoustic radiation and scattering from elastic structures , *Int. J. Numer. Methods Eng.*, **13**, pp.123-138, 1978.
3. H.A. Schenck, Improved integral formulation for acoustic radiation problems, *J. Acoust. Soc. Am.*,**44**, pp.41-58, 1968.
4. A.J. Burton and G. F. Miller, The application of integral equation methods to the numerical solution of some exterior boundary value problems, *Proc. R. Soc. London*, Ser. A 323, pp.201-210, 1971.
5. S. Liapis, Method for suppressing the irregular frequencies from integral equations in water-structure interaction problems, *Comput. Mech.*, **12**, pp.59-68, 1993.
6. P. Bettess, Infinite elements, *Int. J. Numer. Methods*

Eng., **11**, pp.53-64, 1977.

7. J. T. Hunt, M.R. Knittel, C.S. Nichols and D. Barach, Finite-element approach to acoustic scattering from elastic structures, *J. Acoust. Soc. Am.*, **57**(2), pp.287-299, 1975.
8. J.H. Su, V.V. Varadan and V.K. Varadan, Finite element eigenfunction method (FFEM) for elastic wave scattering by arbitrary three-dimensional axisymmetric scatterers, *J. Appl. Mech., ASME*, **51**, pp.1-8, 1984.
10. B. Engquist and A. Majda, Radiation boundary conditions for acoustic and elastic wave calculations, *Comm. Pure Appl. Math.*, **32**, pp.313-357, 1979.
11. A. Bayliss and Eli Turkel, Radiation boundary conditions for wave-like equations, *Comm. Pure Appl. Math.*, **33**, pp.707-725, 1980.
12. D. Givoli and J.B. Keller, Non-reflecting boundary conditions for elastic waves, *Wave Motion* **12**, pp.261-279, 1990.
13. I. Harari and T.J. Hughes, Analysis of continuous formulations underlying the computation of time-harmonic acoustics in exterior domains, *Comput. Methods Appl. Mech. Eng.*, **97**, pp.103-124, 1992.
14. L. Jiang and R. J. Rogers, Effects of spatial discretization on dispersion and spurious oscillations in elastic wave propagation, *Int. J. Numer. Methods Eng.*, **29**, pp.1205-1218, 1990.
15. A. Bossavit and I. Mayergoyz, Edge-elements for scattering problems, *IEEE Trans. Magnetics*, **25**(4), pp.2816-2821, 1989.
16. J. Kim, V.V. Varadan and V.K. Varadan, Finite element modeling of scattering problems involving infinite domains using drilling degrees of freedom, *Comput. Methods Appl. Mech. Eng.*, **134**, pp.57-70, 1996.

▲ Jae-Hwan Kim

Jae-Hwan Kim received the B. S. degree in mechanical engineering from Inha University in 1985, the M. S. degree in mechanical engineering from KAIST in 1987, and Ph. D. degree in engineering science and mechanics from The Pennsylvania State University in 1995.

In March 1996, he joined the Department of Mechanical Engineering at Inha University, Inchon, Korea, where he is an Assistant Professor. Dr. Kim is a member of the editorial board of Smart Materials and Structures journal.

His research interests are finite element modeling and applications of smart structures, and Numerical modeling for infinite domain and fluid-structure interaction problems.